A joint model for boundaries of multiple anatomical parts

Grégoire Kerr[1], Sebastian Kurtek[2] and Anuj Srivastava[2]

[1]INRIA, 2004 Route des Lucioles, 06902 Sophia-Antipolis, France;
[2]Florida State University, Tallahassee, FL 32306 United States

ABSTRACT

The use of joint shape analysis of multiple anatomical parts is a promising area of research with applications in medical diagnostics, growth evaluations, and disease characterizations. In this paper, we consider several features (shapes, orientations, scales, and locations) associated with anatomical parts and develop probability models that capture interactions between these features and across objects. The shape component is based on elastic shape analysis of continuous boundary curves. The proposed model is a second order model that considers principal coefficients in tangent spaces of joint manifolds as multivariate normal random variables. Additionally, it models interactions across objects using area-interaction processes. Using given observations of four anatomical parts: caudate, hippocampus, putamen and thalamus, on one side of the brain, we first estimate the model parameters and then generate random samples from them using the Metropolis-Hastings algorithm. The plausibility of these random samples validates the proposed models.

Keywords: Statistical Shape Analysis, Parameterization Invariance, Configurations of Shapes, Brain Substructures, Spatial Shape Interaction

1. INTRODUCTION

Shape analysis of anatomical parts has proven useful in a variety of medical applications. For example, use of shape analysis helps provide diagnostic tools for tumors and their treatments, and the shapes of brain substructures are contributing in detections of onsets of brain disorders such as Alzheimer and schizophrenia. There are a variety of techniques for shape analysis, depending upon the representations, metrics, and algorithms used. The prominent ideas include active shape models,[1] Kendall's shape analysis[2–4] level set methods,[5] deformable templates, and medial representations.[6] In recent years, there has been a large interest in Riemannian frameworks for shape analysis of curves using stochastic models on infinite-dimensional shape spaces of curves. Although some of these methods allow joint analysis of multiple shapes, the more powerful techniques, especially Riemannian, are primarily restricted to individual shapes. It is clear that anatomical parts seldom occur alone and are influenced by the shapes and other physical attributes of their neighbors. Therefore, any stochastic model of shapes or objects will be more effective if it can incorporate physical attributes, including shapes, of neighboring anatomical parts. Such a model will not only capture the variability manifested in individual shapes but also the interactions between neighboring objects. Modeling multiple shapes has many uses in medical imaging, which include automatic segmentation of brain structures,[7] differentiating between healthy and diseased subjects,[4] and building anatomical atlases. Several past papers have developed joint models for anatomical objects. One such modeling methodology is described in Duta et al.[8] but it is based on discrete sets of landmarks, rather than continuous curves. Others have developed joint shape models using level set methods.[5] Recently, Gorczowski et al.[6] presented multi-object shape analysis using medial representations.

We would like to model shapes as continuous curves and surfaces, while achieving parameterization invariance. This task has been previously explored by Srivastava et al. using a different approach.[9] The idea described in this paper is to extend the framework from Srivastava et al.,[10–12] for modeling single shapes to sets of multiple interacting objects. For simplicity, we will restrict to the 2D objects although, in principle, the ideas extend to 3D objects. In the experiments conducted in this paper, we considered a slice of an MRI of a brain and manually extracted four brain substructures – caudate, hippocampus, putamen, and thalamus, as shown in Figure 1. We used ten such observations as the data, and our goal is to develop a stochastic model that can capture the shapes, positions, locations, and scales manifested in these observations.

2. MATHEMATICAL REPRESENTATIONS

For each of the 2D objects we are going to consider four features: the shape of its contour q, the position of its centroid p, the orientation o, and the length of its contour l. If the boundary of an object is given by a parameterized curve $\beta : [0, 1] \to \mathbb{R}^2$, we can construct these features using:

- position $p = \int_0^1 \beta(t)\ dt \in \mathbb{R}^2$,
- length $l = \int_0^1 \|\dot{\beta}(t)\| dt \in \mathbb{R}_+$,
- orientation $o \in SO(2)$ obtained using the SVD of 2×2 matrix $\int_0^1 (\beta(t)\beta(t)^T) dt$,
- shape $q = \frac{\dot{\beta}(t)}{\sqrt{\|\dot{\beta}(t)\|}}$.

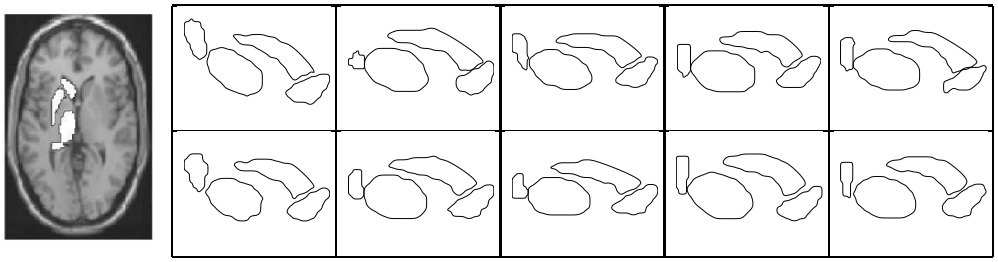

Figure 1. A slice of MRI of human brain showing four anatomical parts: caudate, hippocampus, putamen, and thalamus, on the left side. Right: Ten observations of these parts for different subjects.

2.1 Position

A contour's position, p^j, is defined as being its barycenter $p^j = \int_0^1 \beta^j(t) dt$. This representation, however, is not invariant to global translations. That is, if the whole set (all four objects) is translated, the positions of the individual curves change. In order to avoid this issue the position is computed as a barycenter of the entire set of objects, $p = \frac{1}{4} \sum_{j=1}^4 p^j$. The result of this normalization is evident in Fig. 2.

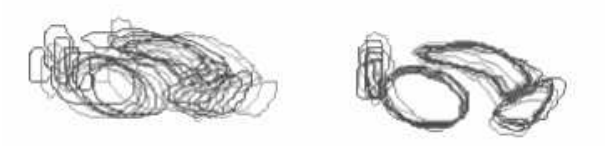

Figure 2. Normalization of objects with respect to position.

2.2 Scale

The scale of an object is its size, which can be quantified using the contour's perimeter. As our original contours are rather "noisy", this might lead to an over-estimation of the curve's scale. In order to avoid this issue, we smooth our input curves using Gaussian smoothing. Thus, the scale of the smoothed contours is given by $s^j = \int_0^1 \|\dot{\beta}^j(t)\| dt$.

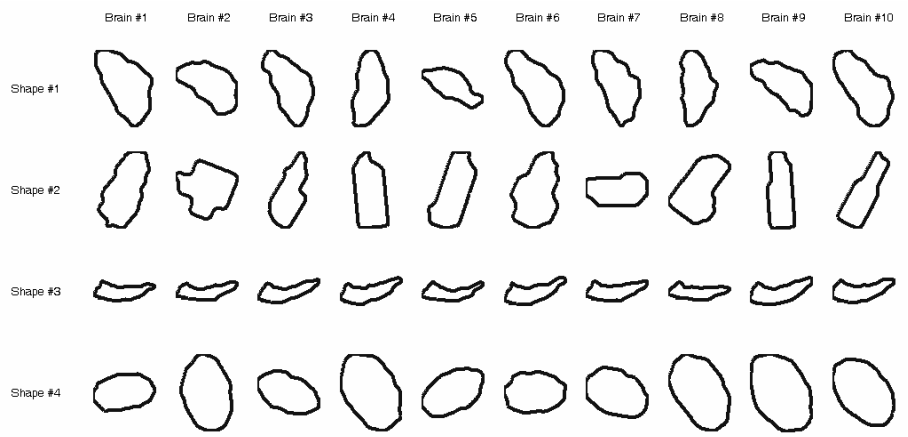

Figure 3. Normalization of contour orientations using averaging of their velocity functions.

2.3 Orientation

A simple way to compute a shape's orientation consists of averaging the orientations of its velocity function, $\dot{\beta}^j$. However, this approach does not provide satisfying results as seen in Fig. 3.

Instead we use a different approach. Assume that the contour $\beta^j(t) = (\beta_x^j(t), \beta_y^j(t))$ has its barycenter equal to the origin. Then compute the matrix A^j as $A^j = \int_0^1 \beta^j(t)\beta^j(t)^T dt$. Using the singular value decomposition we obtain $A^j = V^j \Sigma^j (V^j)^T$. The matrix $V^j \in SO(2)$ provides the orientation of the shape β^j. The result of using this method is displayed in Fig. 4.

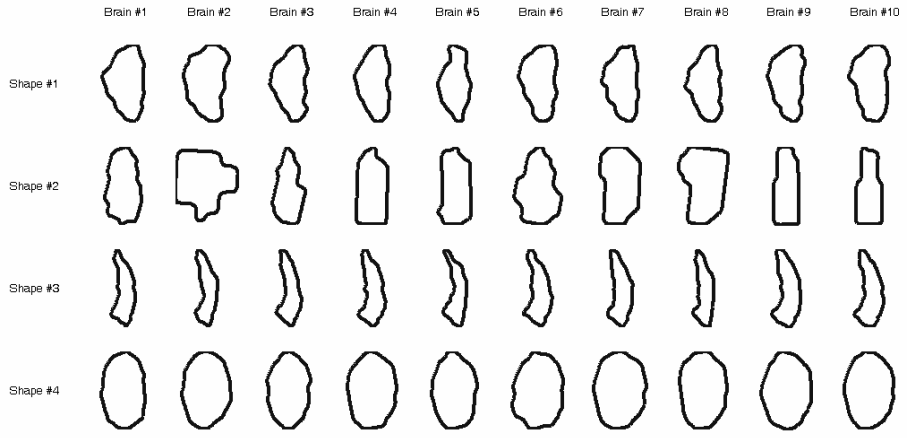

Figure 4. Normalization of contour orientations using singular value decomposition.

2.4 Shape

While the other features follow standard analysis, the analysis of shape requires some more detailed remarks. For shape analysis of closed planar curves, we follow the approach of Joshi et al.[11,12] that defines a shape manifold, imposes a Riemannian metric on it, and uses numerical procedures for computing geodesic paths between arbitrary shapes. *We use the elastic metric that computes an optimal combination of bending and stretching to match points across curves, and leads to shape statistics that better preserve shape features than active shape models or landmark-based shape analysis.* Earlier we have defined a new representation of shape called the square-root velocity function (SRVF) as $q = \frac{\dot{\beta}(t)}{\sqrt{\|\dot{\beta}(t)\|}}$. The condition that the curves are closed

implies that the SRVF q satisfies: $\int_0^1 q(t)\|q(t)\|dt = 0$. Let $\mathcal{C}$ be the set of all closed curves represented by their square root velocity functions. Since shapes are invariant to re-parameterization and rotation, the same shape can be represented by several elements of $\mathcal{C}$. Therefore, let $\mathcal{S}$ denote the shape space, i.e. the quotient space $\mathcal{C}/\left(SO\left(2\right)\times\Gamma\right)$. Here $SO\left(2\right)$ is just the usual notation for the set of 2D rotations while Γ is the set of all re-parameterizations of a unit-length curve. We have now defined a unique representation for the shape of each curve, which allows us to compute statistics on the above mentioned parameters.

3. JOINT MODELS FOR MULTIPLE OBJECTS

3.1 Models for Individual Objects

To start with we summarize a common approach for modeling **shapes** of objects. Since shape spaces are infinite-dimensional nonlinear manifolds, the standard probability models, parametric or nonparametric, do not apply directly. The standard procedure is to compute the sample mean of given shapes on the shape space (e.g. using the notion of the Karcher mean), and to transfer the modeling problem to the tangent space at the mean. Since the tangent space is a vector space, one can perform conventional multivariate statistics in that space. The problem of infinite-dimensionailty is handled by using a relevant finite-dimensional subspace of the tangent space. This subspace can, for example, be obtained using PCA of the observed shapes in that tangent space. Let $q_1,\ldots,q_n$ denote the observed shapes of an anatomical part and let $\mu = \text{argmin}_{q\in\mathcal{S}}\sum_{i=1}^n d([q],[q_i])^2$ be their Karcher mean.[10,12] Here $d(\cdot,\cdot)$ denotes the geodesic distances between shapes in $\mathcal{S}$. Fig. 5 shows the mean shapes of the four anatomical parts studied in this paper. The inverse exponential map $\exp_\mu^{-1}:\mathcal{S}\to T_\mu(\mathcal{S})$ maps individual shapes to the tangent space at the mean. Let $v_i = \exp_\mu^{-1}(q_i)$ be the tangent vectors corresponding to the given shapes, $U_1,U_2,\ldots,U_k$ be the principal singular vectors associated with the $\{v_i\}$ and $\sigma_1^2,\sigma_2^2,\ldots,\sigma_k^2$ be the corresponding singular values. Then,

$$q = \exp_\mu(\sum_{i=1}^k z_i\sigma_i U_i) \quad z_i\sim N(0,1) \tag{1}$$

defines a random shape on $\mathcal{S}$ and the underlying model is called the *wrapped Gaussian distribution*. This is because we have defined a multivariate normal distribution in a subspace of $T_\mu(\mathcal{S})$ and have wrapped it back on the shape space $\mathcal{S}$ using the exponential map.

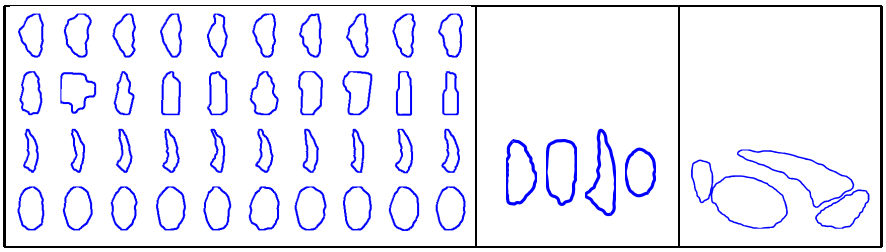

Figure 5. Ten normalized samples for four anatomical parts (left), their Karcher mean shapes in $\mathcal{S}$ (middle) and mean shapes placed at average pose and scales (right).

Since the other features (position, orientation, and scale) are more conveniently specified as Euclidean, we can use any standard model for modeling their variability. In the paper, we have used multivariate normal distributions of these variables. So far we have probability models for the individual features of individual objects.

3.2 Joint Models for Multiple Objects

Now we explore the joint modeling of features across objects and start with the shapes. Let $\mu^1,\mu^2,\ldots,\mu^4$ denote the mean shapes of the four anatomical parts (shown in Fig. 5), and let z_i^j, $j=1,2,\ldots,4$, denote the corresponding random principal coefficients as specified in Eqn. 1. The first step in joint modeling of shapes is to form a random vector $Z=(z_1^1,z_2^1,...,z_k^1,z_1^2,...,z_k^4)$ and impose a multivariate normal density on it. Since the

$4k \times 4k$ covariance matrix of Z contains the cross terms, their model captures some interactions between the shapes of the anatomical parts.

One can model the remaining features in a similar way. Since we have already assumed multivariate models for the other features (scale, translation, and orientation), we can extend them to joint models by considering four times larger vectors for each feature. As an example, consider the modeling of scales of the four objects. We can form a vector of lengths $l = (l^1, l^2, \ldots, l^4) \in \mathbb{R}^4$ and estimate the mean and the covariance of this vector from the given data. These estimated parameters can then be used in a multivariate normal model for the random vector l. We will use π_{sh}, π_p, π_{sc}, and π_o to denote the joint models for shapes, positions, scales, and orientations, respectively, for the four objects. We can control the weights of individual features using the exponents $a = (a_{sh}, a_p, a_{sc}, a_o)$, which take values between 0 and 1 and form a joint probability $\pi \propto \pi_{sh}^{a_{sh}} \cdot \pi_p^{a_p} \cdot \pi_{sc}^{a_{sc}} \cdot \pi_o^{a_o}$. Note that π contains interactions between the same features of the anatomical parts but not interactions between different features. We study this model by generating random samples from π; 16 such random samples are shown in the left side of Fig. 6.

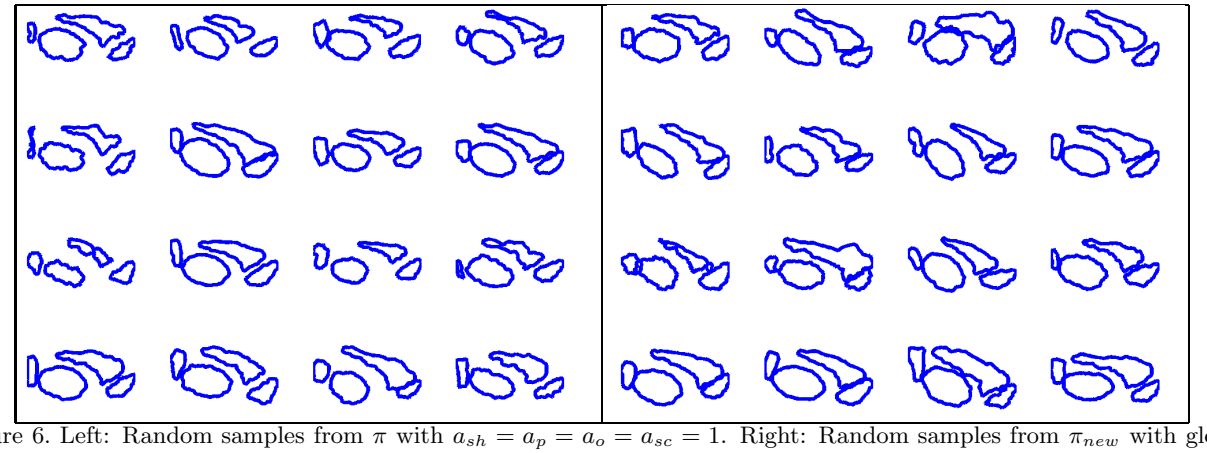

Figure 6. Left: Random samples from π with $a_{sh} = a_p = a_o = a_{sc} = 1$. Right: Random samples from π_{new} with global interactions.

3.3 Models with Global Interactions

In Figure 6 (left) one can see that there still remains a problem in the global organization of the correlated sampled parts: the different parts do not entirely fit together. This problem may be explained by the fact that in π the interactions are only between the same features but not across features. For example, we do not compute any correlations between shapes and positions. As a solution we introduce the following additional terms in our model. To penalize overlaps between objects, we define E_S as the area of the region that belongs to more than one object. To improve relative placements of objects one and three and objects two and four, we first define a "distance" between objects. Let $(t_0, \tilde{t}_0) = argmin_{t,\tilde{t} \in N \times \tilde{N}} \|\beta^j(t) - \beta^{\tilde{j}}(\tilde{t})\|$ where $\|\cdot\|$ is the Euclidean norm, and N, $\tilde{N}$ are neighborhoods of t_0 and $\tilde{t}_0$. We define the global distance between β^j and $\beta^{\tilde{j}}$, $d_m\left(\beta^j, \beta^{\tilde{j}}\right)$, as the mean of $\|\beta^j(t) - \beta^{\tilde{j}}(\tilde{t})\| + \|\beta^{\tilde{j}}(\tilde{t}) - \beta^j(t)\|, (t, \tilde{t}) \in N \times \tilde{N}$ over all t and $\tilde{t}$. We can now define E_{d_1} as $d_m\left(\beta^1, \beta^3\right)$ and E_{d_2} as $d_m\left(\beta^2, \beta^4\right)$. Based on these definitions, we define a global interaction term as $\pi_g = \exp\left(-a \cdot E_S\right) \exp\left(-b \cdot E_{d_1}\right) \exp\left(-c \cdot E_{d_2}\right)$, where we have used $a = 0.01$ and $b = c = 1.2$. The overall joint model for multiple objects is given by: $\pi_{new} = \pi \cdot \pi_g = \pi_{sh}^{a_{sh}} \cdot \pi_p^{a_p} \cdot \pi_o^{a_o} \cdot \pi_{sc}^{a_{sc}} \cdot \pi_g$. Once again, to validate this model, we use random sampling from π_{new}. Although it was possible to directly sample from π earlier, it is no longer feasible to do so due to the global interaction terms. So we use the Metropolis-Hastings algorithm to generate random samples from the overall model π_{new} and some examples are shown in the right side of Fig. 6 . We can see an improvement in relative placements of objects due to the inclusion of the global interaction terms.

4. CONCLUSION

We have proposed a joint model for capturing the observed variability in shapes and other features of multiple anatomical parts. This improves the past work in statistical modeling of shapes of individual objects, represented by continuous closed curves, under an elastic Riemannian framework. This model has two distinct parts. The first involves interactions between the same features across objects, e.g., shapes with shapes and positions with positions, and the second involves more global interactions across features and across objects. We evaluate the model using Metropolis-Hastings based random sampling and determine that the sampled configurations have realistic appearances.

Acknowledgements: This research was supported in part by AFOSR FA9550-06-1-0324, ONR N00014-09-1-0664, NSF DMS-0915003 (AS).

REFERENCES

[1] T. F. Cootes, C. J. Taylor, D. H. Cooper, and J. Graham, "Active shape models: Their training and application," *Computer vision and image understanding* **61**(1), pp. 38–59, 1995.

[2] D. G. Kendall, "Shape manifolds, procrustean metrics and complex projective spaces," *Bulletin of London Mathematical Society* **16**, pp. 81–121, 1984.

[3] I. L. Dryden and K. Mardia, *Statistical Shape Analysis*, John Wiley & Son, 1998.

[4] F. L. Bookstein, "Landmark methods for forms without landmarks: morphometrics of group differences in outline shape," *Medical Image Analysis* **1**(3), pp. 225 – 243, 1997.

[5] S. Hu and D. L. Collins, "Joint level-set shape modeling and appearance modeling for brain structure segmentation," *NeuroImage* **36**(3), pp. 672 – 683, 2007.

[6] K. Gorczowski, M. Styner, J. Jeong, J. Marron, J. Piven, H. Hazlett, S. Pizer, and G. Gerig, "Multi-object analysis of volume, pose, and shape using statistical discrimination," *IEEE TPAMI* **32**(4), pp. 652–666, 2010.

[7] L. H. Staib and J. S. Duncan, "Boundary finding with parameterically deformable models," *IEEE Transactions on Pattern Analysis and Machine Intelligence* **14**(11), pp. 1061 – 1075, 1992.

[8] N. Duta, A. K. Jain, and M. P. Dubuisson-Jolly, "Automatic construction of 2D shape models," *IEEE Transactions on Pattern Analysis and Machine Intelligence* **23**, pp. 433–446, 2001.

[9] A. Srivastava, W. Liu, and S. Joshi, "Modeling spatial patterns of shapes," in *IEEE International Conference on Image Processing*, pp. 1144 –1147, 2008.

[10] A. Srivastava, S. H. Joshi, W. Mio, and X. Liu, "Statistical shape anlaysis: Clustering, learning and testing," *IEEE Trans. Pattern Analysis and Machine Intelligence* **27**(4), pp. 590–602, 2005.

[11] S. H. Joshi, E. Klassen, A. Srivastava, and I. H. Jermyn, "A novel representation for Riemannian analysis of elastic curves in $\mathbb{R}^n$," in *IEEE Conference on Computer Vision and Pattern Recognition (CVPR)*, pp. 1–7, 2007.

[12] A. Srivastava, E. Klassen, S. Joshi, and I. Jermyn, "Shape analysis of elastic curves in Euclidean spaces," *IEEE Trans. Pattern Analysis and Machine Intelligence* **accepted for publication**, 2010.